中國機械工程學刊第四十二卷第四期第 341~351 頁(民國一百一十年)
Journal of the Chinese Society of Mechanical Engineers, Vol.42, No.4, pp. 341~351 (2021)

Establishment and Experimental Verification of Simulation Model of Single-Crystal Silicon Cubic Spline Curve Nanochannel Machining

Zone-Ching Lin *, Xin-Ren Fang **and Jie-Men Ho **

Keywords: atomic force microscopy (AFM), silicon substrate, nanochannel trapezium groove, width, depth, curve

ABSTRACT

The paper proposes a simulation model of Cubic Spline curve nanochannel machining to the expected depth and expected width. Then the paper uses atomic force microscopy (AFM) equipment to make the experimental verification of machining a nanochannel of a straight-line and a Cubic Spline curve to the expected depth and expected width on single-crystal silicon substrate. The paper innovatively proposes using the control point set by the first Cubic Spline curve, and then uses offset equation and the offset amount acquired by the above way to find the calculation method of the control point of Cubic Spline curve equations of other cutting passes on the same cutting layer. Furthermore, the paper calculates the Cubic Spline curve equations of other cutting passes on the same cutting layer. Since AFM equipment cannot carry out Cubic Spline curve machining, the paper proposes applying the calculation equation of the chord height tolerance of Cubic Spline curve and tiny line segment, and further using straight-line approximate Cubic Spline curve method to calculate the straight line of approximate Cubic Spline curve formed by connection of many tiny straight line segments. Also because of the accuracy of AFM equipment being up to 1nm only, we take integers of different intersection points of tiny line segments to carry out machining. In order to reduce the difference, in times of measurement we take the cross-section at the position of the approximate ideal Cubic Spline curve for measurement. Finally, the simulation results of the simulation model established by the paper, with Cubic Spline curve machining performed to the expected width and expected depth, are compared to the AFM experimental results, proving that the simulation model established by the paper is feasible and acceptable.

Paper Received January, 2021. Revised March, 2021. Accepted June, 2021. Author for Correspondence: Zone-Ching Lin.

* *Professor, Department of Mechanical Engineering, National Taiwan University of Science and Technology, No.43, Keelung Rd., Sec.4, Da'an Dist., Taipei City 10607, Taiwan,*
email: zclin@mail.ntust.edu.tw.

** *Graduated Student, Department of Mechanical Engineering, National Taiwan University of Science and Technology, No.43, Keelung Rd., Sec.4, Da'an Dist., Taipei City 10607, Taiwan,*
email:m10803224@mail.ntust.edu.tw,m10503248 @mail.ntust.edu.tw

INTRODUCTION

In recent years, the related scholars have proved that atomic force microscopy (AFM) can be used to perform machining of nano-microstructure on a surface. Therefore, the related scholars explored the measurement and application of AFM. Nanjo et al. (2003) considered the tip of TM-AFM probe as a perfect sphere to carry out simulated small-sphere scanning on an ideal plate under a fixed setpoint value. Lüben et al. (2004) saw probe tip as a perfect sphere, and used contact mode AFM to explore the probe deflection and vertical pressure on a quartz plate. It was proved by the related scholars that applying AFM probe as a machining tool to carry out mechanical cutting was a quite useful technique in machining of nano-microstructures, such as semiconductor, optoelectronic components and metallic surface (2008). Fang et al. (2000) used AFM probe to conduct nano-scratching experiments of silicon substrate coated with an aluminum film. Schumacher et al. (2000) used AFM to carry out mechanical cutting on the surface of heterogeneous structures of GaAs/AlGaAs, and then a single-electron transistor was machined. Yongda et al. (2007) directly used AFM to construct a system similar to computer numerical control (CNC) machining system, and took AFM probe as a cutting tool to carry out scratching of micro-nanostructures on the surface of silicon wafer deposited with copper film. Lin and Hsu (2012) used the theory of specific down force energy (SDFE) to explore the V-shaped groove produced on the sapphire substrate being cut at different downward forces, and explore the method of achieving the expected cutting depth with the fewest cutting passes when cutting a V-shaped groove on each cutting layer for a single cutting pass only. Lin and Yang (2011) used near-field optical lithographic machining Cubic Spline curve and the calculation equation of the chord height tolerance of tiny segments, and further used the method of straight-line approximate Cubic Spline curve to calculate the straight line of approximate Cubic Spline curve formed by connection of many tiny line segments. Cardoso et al. (2018) used the PDMS microfluidics, which contains straight line segments and Cubic Spline curve segments and is manufactured by the copy mode of the premade SU-8 model that was obtained by using lithography, to highly effectively clean the magnetic nanoparticles. Taking the shape of microfluidic flow channel as a reference, the paper carries out research. The above literature did not mention a simulation model, as suggested by the paper, that integrates straight line segment machining with Cubic Spline curve machining on the trapezium groove of nanochannel with two cutting passes offset machining method to the expected width and expected depth, and also did not mention that using AFM machining experiment can prove the simulation model proposed by the paper to be feasible and acceptable.

EXPERIMENTAL EQUIPMENT AND SPECIFIC DOWN FORCE ENERGY MODEL AND EXPERIMENTAL METHOD

Introduction of Experimental Equipment

The AFM machine used in the study is Veeco Instruments Inc.'s Dimension 3100 (D3100), which is equipped at the laboratory of Tungnan University; and the material of the paper's experiments is silicon substrate with diameter 2 inches and thickness 254-304μm, which is provided by Ample Gola International Co., Ltd. The paper uses AFM's diamond-coated probe as a tool to carry out cutting experiment on silicon substrate and for observation. The paper also uses AFM equipment to carry out nanocutting machining and measurement of surface morphology before and after machining. The probe used in experiments is the diamond-coated DT-NCHR probe produced by Nanosensors Inc. The probe tip is like a semi-sphere with a spherical radius of around 150nm. Therefore, when this probe is used for machining of silicon wafer, the probe tip is just like a semispherical cutting tool. The spring constant k_v of the probe provided by the manufacturer is 42 N/m, and its resonance frequency f_v is 320 kHz. In order to obtain a more accurate spring constant k_r of probe, the paper firstly uses tapping mode AFM to find the actual resonance frequency f_r of probe for experiments. It obtains the value of f_r is 309.6 kHz. Besides, since the spring constant k_r of probe in the experiments can be obtained from the equation $k_r = (f_r^2 \times k_v)/f_v^2$, the actual spring constant k_r of probe in the experiments can be acquired from the resonance frequency f_v and spring constant k_v of probe provided by the manufacturer. It obtains the value of k_r is 39.3 N/m.

Measurement Method of the Downward Force of AFM Probe

The force-distance Cubic Spline curve explains the relationship between setpoint value and offset amount of the probe cantilever. Before conducting the experiment, the paper firstly sets different setpoint values for AFM machine under the contact model, and uses different setpoint values to measure the offset amount d of probe cantilever, and then substitutes the offset amount of probe cantilever in equation (1) to acquire the corresponding downward force value F_d of this setpoint. In equation (1), k_r is the actual spring constant of probe.

$$F_d = k_r d \tag{1}$$

SDFE Theoretical Model and SDFE Calculation Method

The paper applies specific down force energy (SDFE) as the fixed value, and uses AFM experiment to calculate the SDFE of the machined single-crystal silicon substrate. SDFE is defined as follows: Let the energy produced by the machined downward force applied by the cutting tool of probe onto the workpiece multiply the cutting depth, and then divide the volume removed from workpiece by the cutting tool due to downward force. The equation of SDFE is shown in equation (2):

$$\text{SDFE (specific down force energy)} = \frac{F_d \times \Delta d_n}{\Delta V_n} \tag{2}$$

Here, F_d denotes the downward force applied by cutting tool onto the workpiece; Δd_n denotes the increased cutting depth for cutting at the nth cutting pass on the cutting layer; and ΔV_n denotes the volume removed from the cut workpiece at the nth cutting pass. Since the volume removed from workpiece by cutting changes with the increase of cutting depth, ΔV_n is the function of cutting depth Δd_n. From the moving of cutting tool to the cutted groove, the depth in the middle area gradually inclines to be at a fixed cutting depth. As to the volume removed by downward force after moving of cutting tool, due to cutting in the abovementioned process, the volume of the distance of the radius R behind the cap of workpiece being cutted in by the probe in advancing direction has been removed. Therefore, at this moment, the removed volume at the 1st cutting pass on the 1st cutting layer is half of the spherical cap volume under the cutting depth Δd_1, and the removed volume ΔV_1 is shown as follows:

$$\Delta V_1 = \frac{1}{2}\pi \Delta d_1^{\,2}\left(R - \frac{\Delta d_1}{3}\right) \tag{3}$$

where R denotes the radius of the tip of the cutting tool of probe; and Δd_1 denotes the cutting depth of the 1st cutting pass on the 1st cutting layer.

As to the volume removed by downward force at the 1st cutting pass on the 2nd cutting layer, since the groove is removed at the 1st cutting pass on the 1st cutting layer, the removed volume is just like an arc wedge. Therefore, for the geometric shape of cutting tool and the cutting depth, the paper uses CATIA's CAD software to make a solid model in order to carry out simulation and calculation of the volume removed by the downward force at 1st cutting pass on the 2nd cutting layer. The paper uses CAD software to construct and calculate such a removed volume. The paper applies an important concept that for the removed volume of SDFE with the probe at the (i+1)th position, it is supposed that the AFM probe moves from the ith position for a distance of cap radius of the probe cutting into the workpiece. CAD software is also used to calculate this removed volume. Therefore, the paper applies a certain downward force to have action on workpiece. The paper also uses the radius of probe tip and the depth of cutting to calculate the volume removed from workpiece at the stable cutting depth during the 1st cutting pass on the 1st cutting layer, and employs CAD for simulation and calculation of the volume removed from workpiece during multiple cutting passes on multiple cutting layers. The paper uses straight-line machining of groove at the 1st cutting pass on the 1st cutting layer using different downward forces. When using SDFE concept to carry out calculation, it can be found that SDFE value inclines to be a fixed constant $0.01775\left({\mu N \cdot \mathrm{nm}}/{nm^3}\right)$.

TWO CUTTING PASSES OFFSET MACHINING METHOD OF TRAPEZIUM GROOVE ON NANOCHANNEL

The two cutting passes offset machining method of trapezium groove on nanochannel is explained as follows. First of all, it is set that under a fixed cutting depth on each cutting layer, the cutting depth at the 1st cutting pass is firstly cut. After that, the probe is offset rightwards to cut the workpiece at the 2nd cutting pass on this cutting layer. During this time the cutting depth at the 2nd cutting pass on this cutting layer has the same cutting depth as the 1st cutting pass. In this way, between the shape of the cut cross-section before probe offset and the shape of the cut cross-section of trapezium groove nanochannel bottom at the two cutting passes after probe offset, there is an upward height H at the bottom, as shown in Figure 1.

If this upward height H at the bottom of trapezium groove nanochannel exceeds the set convergence value of upward height at the bottom, the probe should be offset step by step to carry out cutting. After step-by-step offset of the probe, the upward height H at the bottom at the two cutting passes of machining is made to converge to within a range. In order to make the trapezium groove's bottom on straight-line nanochannel have a result closer to a plane after cutting at the bottom, the paper sets the range of numerical value of the upward height at the bottom to be a numerical value with the surface roughness of single-crystal silicon substrate at below 0.54nm. Right then, it is supposed that the probe offset amount required for cutting of trapezium groove nanochannel has been achieved.

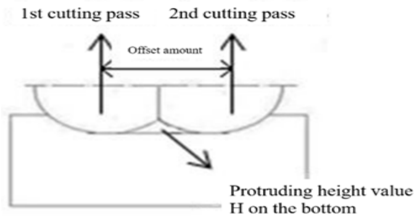

Figure 1 Schematic diagram of protruding height value H on the bottom of trapezium groove between two cutting passes

During this time, after the probe is offset, substitute the SDFE value obtained from AFM experiment in SDFE equation (2). Since ΔV_n in equation (2) is the function of Δd_n, which is the same cutting depth at the 1st cutting pass on this layer. Since the radius of AFM probe has been known, CAD software can be used to find ΔV_n. After inverse induction from equation (2), the required downward force for machining trapezium groove at the 2nd cutting pass on this cutting layer after probe offset can be acquired. The above theoretical model is that after the cutting tool of probe offsets laterally on this cutting layer, which is set to have the same cutting depth, SDFE concept is employed to simulate the downward force of the laterally offset probe that needs to be changed during probe cutting of workpiece at the 2nd cutting pass on this cutting layer.

ESTABLISHMENT OF MACHINING METHOD OF TRAPEZIUM GROOVE ON STRAIGHT LINE SEGMENT NANOCHANNEL TO THE EXPECTED DEPTH AND EXPECTED WIDTH

The paper establishes the machining method of trapezium groove on straight line segment nanochannel to the expected depth and expected width. According to the method established by the paper, we can decide the required number of cutting passes n for machining of trapezium groove nanochannel to the expected depth and expected width, total offset amount P_{total} of probe between cutting passes, probe offset amount P_n between two adjacent cutting passes, and the upward height H at the bottom produced between two adjacent cutting passes.

First of all, set the numerical values of the expected depth and expected width for machining of trapezium groove on straight line segment nanochannel to the last cutting layer, as shown in Figure 2. Figure 2 shows the schematic diagram of 3 cutting passes. In Figure 2, d_e denotes the expected depth for cutting to the last trapezium groove on straight line segment nanochannel; w_e denotes the expected width for machining to the last trapezium groove on straight line segment nanochannel; P_{total} denotes the total offset amount of probe; P_n denotes the probe offset amount at two adjacent cutting passes; H denotes the upward height at the bottom; and z denotes the horizontal distance from the center of probe to the connected place between probe and the edge of trapezium groove.

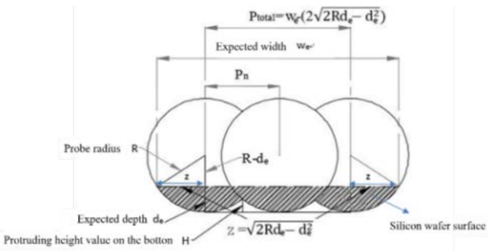

Figure 2 Schematic diagram of geometric relationship in fabrication of nanochannel trapezium groove on straight line segment to the expected width and expected depth (3 cutting passes)

If the probe tip radius R is known, the equation of Pythagorean theorem can be used to derive equation z in Figure 2 as follows:

$$\because\ z^2 + (R - d_e)^2 = R^2$$

$$\therefore\ z = \sqrt{2Rd_e - {d_e}^2} \tag{4}$$

From Figure 2, it can be seen that there is z by both the left and right sides at the farthest cutting pass, so that $2z = 2\sqrt{2Rd_e - {d_e}^2}$. In order to obtain the required total offset amount of probe, equation (5) of total offset amount of probe can be derived from Figure 2 as follows:

$$P_{total} = w_e - (2\sqrt{2Rd_e - {d_e}^2}) \tag{5}$$

As seen from equation (5), when the last expected depth and expected width of trapezium groove on straight line segment nanochannel have been known, the total offset amount of probe can be acquired from equation (5). During this time, we further find that after calculation of total offset amount of probe, the probe offset amount P_n at two adjacent cutting passes is the main key point affecting the upward height H of trapezium groove. The paper derives the equation of probe offset amount P_n at two adjacent cutting passes and the equation of upward height H at the bottom between two adjacent cutting passes, as shown in equation (6) and equation (7) respectively below. Figure 3 shows the schematic diagram of probe offset amount P_n at two adjacent cutting passes and upward height H at the bottom of trapezium groove nanochannel.

As known from Figure 2 and Figure 3, H is the upward height at the bottom of trapezium groove nanochannel produced between two adjacent cutting passes; P_n is the probe offset amount between two adjacent cutting passes; and the n in P_n represents the number of cutting passes on each cutting layer. If there are two cutting passes only, the n in P_n is 2, and $P_n = P_2$. Therefore, from Figure 2 and Figure 3, P_n and H equations can be derived and expressed as equations (6) and (7) as follows:

$$P_n = \frac{P_{total}}{n-1} \tag{6}$$

$$H = R - \sqrt{R^2 - (\frac{P_n}{2})^2} \tag{7}$$

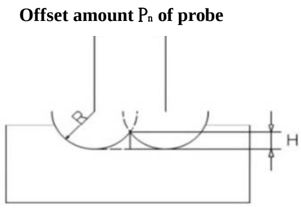

Figure 3 Schematic diagram of probe offset amount P_n at two adjacent cutting passes and upward height H at the bottom

From equation (5), we can calculate the required total offset amount P_{total} of probe for machining of trapezium groove nanochannel to the expected depth and expected width. If each cutting layer is divided into n cutting passes for cutting, equation (5) can be used to calculate the total offset amount P_{total}. According to equation (6), we can calculate the probe offset amount P_n of two adjacent cutting passes required to reach the expected depth and expected width of trapezium groove nanochannel. After we have obtained the probe offset amount P_n of two adjacent cutting passes on each cutting layer, we also have to substitute this P_n value in equation (7) to calculate the upward height H at the bottom, and then observe the selected number of cutting passes, and check whether the upward height H at the bottom has exceeded the convergence value 0.54nm.

ESTABLISHMENT OF SIMULATION MODEL OF NANOCHANNEL THAT INTEGRATES STRAIGHT LINE SEGMENT WITH CUBIC SPLINE CURVE SEGMENT MACHINING TO THE EXPECTED DEPTH AND EXPECTED WIDTH

Regarding the paper's nanochannel that integrates straight line segment with Cubic Spline curve segment machining to the expected depth and expected width, straight line segment machining is carried out first, and then Cubic Spline curve segment machining is carried out later. In the integration process, since the machining from the straight line segment to the Cubic Spline curve segment is continuous, the downward force, offset amount, number of cutting passes and number of cutting layers used for ideal Cubic Spline curve segment machining at each cutting pass are the same as those of straight line segment machining. When the cutting tool enters the Cubic Spline curve segment from the straight line segment, equation of the Cubic Spline curve has to be decided first. Therefore, the equation of an ideal Cubic Spline curve segment at each cutting pass has to be derived first.

However, the smallest resolution achieved in machining by AFM machine is 1nm only. Thus, we have to obtain the line segments of approximate Cubic Spline Cubic Spline curves from different ideal Cubic Spline Cubic Spline curves. The method of obtaining these line segments of approximate Cubic Spline Cubic Spline curves is through chord height tolerance equation, and to make the chord height tolerance less than 0.5nm.

Establishment of Cubic Spline Curve Equation of Ideal Cubic Spline Curve Machining

The steps for establishment of Cubic Spline curve equation of ideal Cubic Spline curve machining are as follows:

1. The ideal curve used by the paper is cubic spline Cubic Spline curve, and its equation is:

$$y= a_0+a_1x+a_2x^2+a_3x^3 \text{,} \tag{8}$$

where x denotes the x coordinate of the Cubic Spline curve; and y denotes the y coordinate of the Cubic Spline curve.

From the farthest periphery of the path of machining to be made, the paper starts setting the positions of the 4 expected control points.

2. Enter the positions of the 4 control points, (x_1, y_1), (x_2, y_2), (x_3, y_3) and (x_4, y_4), to achieve 4 simultaneous equations as follows:

$$y_1 = a_0 + a_1x_1 + a_2x_1^2 + a_3x_1^3$$
$$y_2 = a_0 + a_1x_2 + a_2x_2^2 + a_3x_2^3$$
$$y_3 = a_0 + a_1x_3 + a_2x_3^2 + a_3x_3^3$$
$$y_4 = a_0 + a_1x_4 + a_2x_4^2 + a_3x_4^3$$

After solving the simultaneous equations, a_0, a_1, a_2 and a_3 are acquired. Hence, a Cubic Spline curve equation $y= a_0 + a_1x + a_2x^2 + a_3x^3$ is acquired.

Establishment of Cubic Spline Curve Equations of Different Cutting Passes After Offset

Establish Cubic Spline curve equation of the second cutting pass after offset. The offset amount during offset this time is the simulated offset amount of straight line segment machining obtained from the step aforesaid. After that, according to the offset amount of the straight line segment at the 2nd cutting pass, we carry out offset for the 4 control points of the 1st Cubic Spline curve already established, and then use the positions of the 4 control points after offset to establish a Cubic Spline curve equation of the 2nd cutting pass.

The Cubic Spline curve equation of the 1st cutting pass is $y = a_0 + a_1x + a_2x^2 + a_3x^3$. The slope of any single control point $P(x_i, y_i)$ of the 4 control points is:

$$m = \frac{dy}{dx} = f'(x_i) = a_1 + 2a_2x_i + 3a_3x_i^2 \quad i = 1,2,3,4 \tag{9}$$

The tangent line going through the 1st control point also goes through $P(x_1, y_1)$; and the straight line with its slope being m is:

$$y_{t1} = y_1 + m(x_{t1} - x_1)$$

The normal line going through the 1st control point just goes through $P(x_1, y_1)$; and the straight line being perpendicular to the tangent line is:

$$y_{n1} = y_1 - \frac{1}{m}(x_{n1} - x_1)$$

In order to let the normal line, which goes through $P(x_1, y_1)$ after offset, be able to go through the first control point $Q(x_{a1}, y_{a1})$ of the Cubic Spline curve equation at the 2nd cutting pass, the distance between the control point $Q(x_{a1}, y_{a1})$ and the control point $P(x_1, y_1)$ is d. It is known that the slope of the straight line of this normal line is $\frac{1}{m}$. According to the concept of similar triangles (with the length of the corresponding sides being proportional), it is known that:

$$\frac{x_{a1}-x_1}{m} = \frac{y_{a1}-y_1}{1} \tag{10}$$

According to Pythagoras theorem, it is known that:

$$d^2 = (x_{a1} - x_1)^2 + (y_{a1} - y_1)^2 \tag{11}$$

Let equations (10) and (11) become simultaneous equations, and then the following equations are obtained:

$$y_{a1}=y_1+\sqrt{\frac{d^2}{1+m^2}} \tag{12}$$

$$x_{a1}=x_1+m \times \sqrt{\frac{d^2}{1+m^2}} \tag{13}$$

Then, the position of the first control point $Q(x_{a1}, y_{a1})$ required for the Cubic Spline curve equation of the 2nd cutting pass can be known. Following the above steps and the way of offset, the remaining 3 control points can all be calculated. Another 3 control points of the Cubic Spline curve at the 2nd cutting pass can be obtained. Calculate these control points according to the above calculation method of the Cubic Spline curve equation for calculation of ideal Cubic Spline curve machining. Then the Cubic Spline curve equation of the 2nd cutting pass can be established.

Establishment of Line Segment for Tiny Straight-Line Approximate Cubic Spline Curve

The paper establishes line segment for tiny straight-line approximate Cubic Spline curve, and the establishment method is explained below.

When multiple tiny straight-line segments are used to approximate the Cubic Spline curve of machining parameter, the chord height tolerance (being the vertical distance between line segment and Cubic Spline curve of path) is usually used to serve as a reference for measurement of difference in shape between the path of line segment and the shape of Cubic Spline curve. Yeh and Hsu, (2002) used the concept of restricted chord height tolerance to carry out planning of the path of Cubic Spline curve machining. From the relationship between the allowable maximum chord height to tolerance ($d_{\text{all max}}$) and the geometric radius (ρ) of approximate Cubic Spline curve, Yeh and Hsu, (2002) obtained the length of tiny straight line segment, from which the next intersection point on the Cubic Spline curve can be estimated.

The equation for calculation of chord height tolerance is as follows (Yeh and Hsu, 2002):

$$d_{\text{all max}}=\rho_i-\sqrt{\rho_i-(\frac{L_i^{Arc}}{2})^2} \tag{14}$$

where: $d_{\text{all max}}$ denotes the supposed allowable maximum chord height tolerance. When this value is smaller, it implies that the machining path is closer to the machining Cubic Spline curve. L_i^{Arc} denotes the length of the i^{th} straight line segment obtained from calculation by approximate Cubic Spline curve.

Meanwhile, when the engineering function y = f(x), its curvature is $k = \frac{|f''(x)|}{(1+[f'(x)]^2)^{\frac{3}{2}}}$, and geometric radius is $\rho = \frac{1}{k}$. Therefore, when cubic spline Cubic Spline curve equation is used to describe the Cubic Spline curve, the geometric radius of the i^{th} line segment is:

$$\rho_i=\frac{(1+[f'(x)]^2)^{\frac{3}{2}}}{|f''(x)|} \tag{15}$$

where ρ_i denotes the geometric radius of the i^{th} line segment. Equation (15) can be used to achieve the geometric radius size of approximate Cubic Spline curve. Substitute it in equation (14), and then the length L_i^{Arc} of the i^{th} straight line segment of straight-line approximate Cubic Spline curve can be obtained, and its equation is as follows:

$$L_i^{\text{Arc}}= 2\sqrt{\rho_i-(\rho_i-d_{\text{all max}})^2} \tag{16}$$

From equation (16), the length L_i^{Arc} of the i^{th} straight line segment of straight-line approximate Cubic Spline curve can be obtained. Meanwhile, the length L_i^{Arc} can be used to estimate the $(i+1)^{\text{th}}$ intersection point Q_{i+1} on the Cubic Spline curve. Since the Cubic Spline curve at the farthest periphery has the greatest radius of curvature, when it gets closer to the inner side, the acquired radius of curvature of the Cubic Spline curve would be smaller, and thus the calculated chord height tolerance would also be smaller. Therefore, we start calculation from the Cubic Spline curve at the farthest periphery so as to more conveniently control our expected chord height tolerance.

VERIFICATION METHOD OF SIMULATION AND MEASUREMENT OF AFM MACHINING EXPERIMENT

In order to verify that the simulation model of nanochannel that integrates straight line segment with Cubic Spline curve segment machining to the expected depth and expected width, as established by the paper, is feasible and acceptable, the paper further establishes the verification method of simulation and measurement of AFM machining experiment. The verification steps of simulation and measurement of AFM machining experiment are as follows:

1. Regarding verification of straight line segment, we use the simulated result of straight line segment to carry out verification. Take a cross-section from the straight line segment to carry out measurement.
2. For the first example of two cutting passes, the measured cross-section of the ideal line segment is the position of straight line formed by connecting the control points of the 1st cutting pass with those of the 2nd cutting pass. Since two points can determine a line, we can suppose that the equation is y = ax+b. Substitute the two known points of the position in the simultaneous equations to find the solutions. Then the straight line equation of the measured cross-section of the ideal line segment can be obtained. For the initial point and end point of each known tiny line segment, the above two points are used to determine the calculation method of a line. Then the equation of straight line of tiny line segments at the 1st cutting pass and the 2nd cutting pass can be acquired.
3. Take the tiny straight line segments of approximate Cubic Spline curve at the 1st cutting pass and the tiny line segments at the 2nd cutting pass. The equation of straight line of the cross-section of the ideal line segment would intersect with the tiny straight line segments of approximate Cubic Spline curve at the 1st cutting pass and the tiny straight line segments at the 2nd cutting pass at one point respectively. Use the straight line equation achieved in Step 2 to form simultaneous equations. Then the positions of two points where approximate Cubic Spline Cubic Spline curves intersect can be obtained. After that, confirm whether the two intersection points are both on the tiny straight line segments of approximate Cubic Spline curve at the 1st cutting pass and the tiny straight line segments at the 2nd cutting pass, so as to avoid an excessively great difference between the compared position and the calculated position during the subsequent comparison.
4. Calculate again the distance between the two intersection points formed between the tiny straight line segments of approximate Cubic Spline curve at the 1st cutting pass and the tiny straight line segments at the 2nd cutting pass. Such a distance is just the offset amount of approximate Cubic Spline curve of the two tiny straight line

segments at the 1st cutting pass and the 2nd cutting pass.

5. Carry out simulation according to the various fixed downward forces set for tiny straight line segments at different cutting passes during straight line machining of approximate Cubic Spline curve as well as the offset amount of two tiny straight line segments calculated in Step 4. Then the simulated width, depth and upward height of the cross-section at the measurement positions of two tiny straight line segments can be acquired. They are compared to the width, depth and upward height of the cross-section at the same measurement positions of AFM experiment. Then the difference in line segment of approximate Cubic Spline curve between simulation and AFM experiment can be achieved.
6. At the position of around the middle of the tiny straight line segment of approximate Cubic Spline curve at the 1st cutting pass in Step 2, just at above the position of around the nearest maximum chord height tolerance value, select a point on the first ideal Cubic Spline curve. At this point, calculate the equation of the normal line perpendicular to the 2nd ideal Cubic Spline curve, and achieve the intersection point with the 2nd ideal Cubic Spline curve. The equation of this straight line of normal line is just the equation of straight line of the cross-section to be measured by us. This equation and the straight line equation of tiny straight line segments of approximate Cubic Spline curve at the 1st cutting pass and the 2nd cutting pass calculated in Step 3 form simultaneous equations. After solving them, we can obtain the position of the intersection point between the tiny straight line segment of approximate Cubic Spline curve segment at the 1st cutting pass and the tiny straight line segment at the 2nd cutting pass and the straight line equation of the measured cross-section. After that, calculate the distance between the positions of two intersection points at two cutting passes calculated in Step 4. Such a distance is just the offset amount of two intersection points where two tiny straight line segments intersect with the equation of straight line of the measured cross-section. After that, this offset amount is used to carry out simulation, and then we can achieve the width, depth and upward height simulated on the cross-section at two cutting passes between two tiny straight line segments at around the middle position of approximate Cubic Spline curve. These achieved results are compared to the width, depth and upward height of the cross-section measured in the AFM experiment that measures the same measured cross-section. Then the difference between the simulation and the ADM experiment can be obtained.
7. If the value of difference between them is small, it can be proved that the simulation model of nanochannel that integrates straight line segment with Cubic Spline curve segment machining to the expected depth and expected width, as established by the paper, is feasible.

SIMULATION RESULTS AND EXPERIMENTAL VERIFICATION

Exploration of Simulation of Straight Line Segment to The Expected Depth and Expected Width

The shape of trapezium groove nanochannel that integrates straight line segment with Cubic Spline curve segment machining, as explored in the paper, refers to the microfluid system of Cardoso et al. (2018), as shown in Figure 6 below. In Figure 6, the nanochannel contains straight line segment and Cubic Spline curve segment. Referring to Figure 6, the schematic diagram of the nanochannel used in the paper for machining is shown in Figure 7 below.

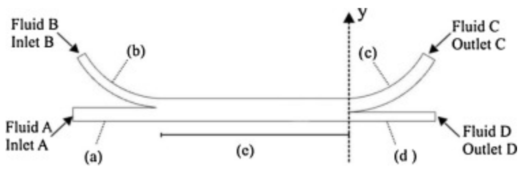

Figure 6 Microfluid system (Cardoso et al., 2018)

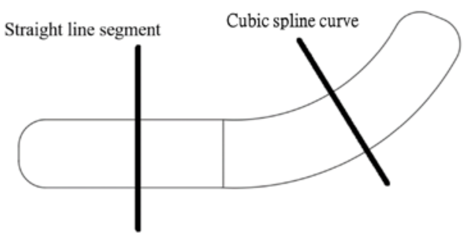

Figure 7 Schematic diagram of nanochannel for machining

Calculation of Offset Amount, Number of Passes and Upward Height with the Straight-Line Segment Reaching Different Expected Depths and Expected Widths

Using the above calculation method, it can be calculated that when the depth is 30nm, the width is 202nm, the offset amount is 22nm and the number of cutting passes is 2 cutting passes, then the upward height is 0.404nm, which is converged at below the set target convergence value 0.54nm, as shown in Figure 8 below.

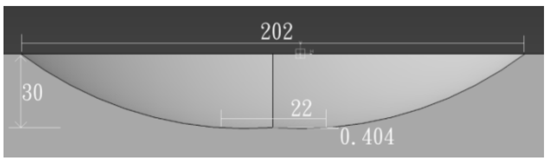

Figure 8 Diagram of simulation results at 2 cutting passes under the expected depth 30nm and the expected width 202nm

Exploration and Simulation of Cutting Layer

After the paper uses the calculated offset amount of straight line segment, number of offset cutting passes and upward height, downward force is substituted to carry out simulation. It is known that the maximum allowable downward force is 137μN. For safety sake, and for prevention of breaking of the probe for being fatigue after cutting for multiple times, we set the least safety coefficient to be 1.5. Under the safety coefficient of 1.5, the maximum downward force is 91.33μN, and its depth can reach 23.014nm only. Therefore, to achieve the target depth at a deeper depth, the number of cutting layers has to be increased.

Using the above calculation method of number of cutting passes, offset amount and upward height after machining of the nanochannel to the expected depth and expected width, we can make calculation that when the expected depth is 30nm and the expected width is 202nm, the offset amount is 22nm, the number of cutting passes is 2 cutting passes, and the upward height at the bottom is 0.404nm. The downward force used on the 1st cutting layer is 91.33μN. As known from the simulation results, the cutting depth is 23.014nm only. Therefore, the paper adds one more cutting layer. On the 2nd cutting layer, the downward force at the 1st cutting pass is 34.92μN; and the downward force at the 2nd cutting pass is 19.88μN. The simulated depth is 30.006nm; width of opening is 202.016nm; offset amount is 22nm, and upward height at the bottom is 0.404nm.

Establishment of Simulation Model of Nanochannel that Integrates Straight Line Segment with Cubic Spline Curve Segment Machining to the Expected Depth and Expected Width

As mentioned above, the nanochannel integrates straight line segment with Cubic Spline curve segment machining to the expected depth and expected width. Its process is that straight line segment is machined first, and Cubic Spline curve segment is machined later. In the integrated machining process, since the machining from straight line segment machining to Cubic Spline curve segment machining is continuous, the downward force, offset amount, number of cutting passes and number of cutting layers used for ideal Cubic Spline curve segment machining at each cutting pass are the same as those of straight line segment. When the cutting tool enters the Cubic Spline curve segment from the straight line segment, equation of the Cubic Spline curve has to be decided first. Therefore, the equation of an ideal Cubic Spline curve segment at each cutting pass has to be derived first.

However, the smallest resolution achieved in machining by AFM machine is 1nm only. Thus, we have to obtain approximate Cubic Spline Cubic Spline curves from different ideal Cubic Spline Cubic Spline curves. The method of obtaining the line segments of these approximate Cubic Spline Cubic Spline curves is through chord height tolerance equation, and to make the chord height tolerance less than 0.5nm. Therefore, the next section will explain the establishment process of Cubic Spline curve equation of ideal Cubic Spline curve machining, and the establishment process of line segment of tiny straight-line approximate Cubic Spline curve. After that, the paper establishes the AFM-measured cross-section to carry out verification of the simulation results and AFM machining experiment.

Calculation of Ideal Cubic Spline Curve Equations of the 1st Cutting Pass and the 2nd Cutting Pass

When calculating the Cubic Spline curve of ideal Cubic Spline curve segment at the 1st cutting pass, we take these 4 control points: (0,0), (255,55), (425,245) and (500,400). The unit of 4 control points in nm. According to the foregoing calculation steps of ideal Cubic Spline curve, the equation of ideal Cubic Spline curve at the 1st cutting pass is calculated: $y_1=0.000004x^3 - 0.00005x^2 + 0.0896x$.

As known from the simulation results aforesaid, under the expected depth 30nm and the expected width 202nm, the offset amount of straight line segment at the 2nd cutting pass is 22nm. According to the foregoing calculation steps for calculation of ideal Cubic Spline curve at the 2nd cutting pass, the equation of ideal Cubic Spline curve at the 2nd cutting pass after offset is calculated: $y_2=0.000004x^3 - 0.00001x^2 + 0.0309x + 21.973$.

Establishment of Line Segment of Approximate Cubic Spline Curve of Tiny Straight Lines

As mentioned above, we calculate the line segment of approximate Cubic Spline curve of tiny straight line segment of an approximate ideal Cubic Spline curve. After the coordinates of the various tiny straight line segments at different cutting pass are acquired, since the smallest resolution achieved in machining by AFM machine is 1nm only, we firstly take the integer value, at the accuracy of 1nm, for the numerical value of line segment of approximate Cubic Spline curve having decimal point, and then acquire the line segment of approximate Cubic Spline curve formed by the new tiny straight line segments being integers. When machining of the line segment of approximate Cubic Spline curve formed by tiny straight line segments is functioned on AFM machine, the coordinates of the line segments of approximate Cubic Spline curve at the 1st cutting pass after acquisition of integer values are shown in Figure 9 below. The coordinates of the line segments of approximate Cubic Spline curve at the 2nd cutting pass after acquisition of integer values are shown in Figure 10 below.

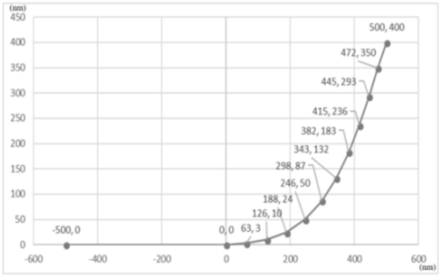

Figure 9 Coordinates of the various tiny straight line segments of the line segment of approximate Cubic Spline curve at the 1st cutting pass after acquisition of integer values

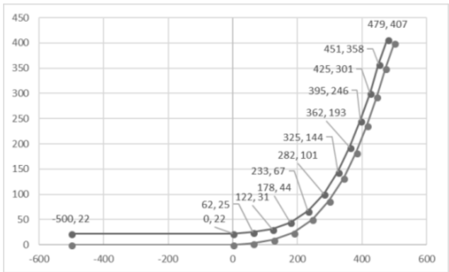

Figure 10 Coordinates of the various tiny straight line segments of the line segment of approximate Cubic Spline curve at the 2nd cutting pass after acquisition of integer values

Measured Cross-Section and Offset Amount in AFM Machining Experiment

Regarding the measured cross-section in AFM machining experiment, according to the calculation steps aforesaid, we take a measured cross-section on the straight line segment, and 4 measured cross-sections on the Cubic Spline curve segment, as shown in Figure 11 below. After calculation, the equation of straight line segment of the measured cross-section in proper order as shown in Figure11 is the equation of the measured cross-section of straight line: $y_1 = x + 250$; and the equations of 4 measured cross-sections of the Cubic Spline curve segment in proper order2,3,4and5 as shown in Figure11 are: $y_2 = -0.8847x + 351.5634$; $y_3 = -0.7774x + 353.296$; $y_4 = -0.4119x + 476.736$; and $y_5 = -0.387x + 491.735$. The offset amount of each measured cross-section is the offset amount of straight line segment being 22nm; and the offset amounts of the 4 measured cross-sections of the Cubic Spline curve segment are 21.254nm, 21.379nm, 21.537nm and 21.704nm. Figure 11 is the diagram of cross-section positions of the measured cross-sections.

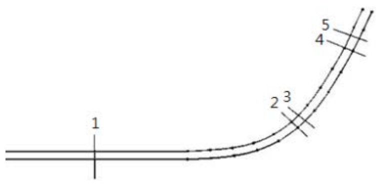

Figure 11 Diagram of cross-section positions of the measured cross-section

After the above acquisition of the offset amounts of different measured cross-sections, we can start to verify the simulation results and experimental results of the nanochannel that integrates straight line segment with Cubic Spline curve segment machining to the expected depth and expected width.

Verification of Measurement of Simulation Results and AFM Machining Experimental Results of the two Cutting Passes when Machining is Up to the Expected Depth 30nm and the Expected Width 202nm

After achieving the equations and offset amounts of different measured cross-sections, we start carrying out simulation of the nanochannel that integrates straight line segment with Cubic Spline curve segment machining to the expected depth and expected width; and simulated calculation is made for the width of opening, depth and upward height on different cutting layers at different cutting passes. SDFE method is also used to calculate the downward force on two cutting layers at the 1st cutting pass and the 2nd cutting pass. After that, we carry out verification of AFM experiment. The comparative results between the simulation results and the measurement results in AFM machining experiment are shown in Table 1.

Table 1 Comparison between simulation results and experimental results on the 2nd cutting layer at the 2nd cutting pass under the expected depth 30nm and the expected width 202nm

2st cutting layer	Downward force (μN)	Cutting pass	Experimental cutting depth(nm)	Simulated cutting depth(nm)	Difference in cutting depth	Offset amount (nm)	Experimental upward height (nm)	Simulated upward height (nm)	SDFE value ([illegible])	Experimental width of opening (nm)	Simulated width of opening (nm)	Difference in width of opening
1st measured cross-section (straight line segment)	34.92	1st cutting pass	30.045(1)	30.006(1)	0.130%	22.000	0.401(1)	0.404(1)	0.01775	202.049	202.016	0.016%
	19.88	2nd cutting pass	30.045(2)	30.006(2)	0.130%		0.401(2)	0.404(2)	0.01775			
2nd measured cross-section (curve segment)	34.92	1st cutting pass	30.109(1)	30.048(1)	0.203%	21.254	0.338(1)	0.327(1)	0.01775	201.563	201.52	0.021%
	19.88	2nd cutting pass	30.224(2)	30.152(2)	0.238%		0.427(2)	0.431(2)	0.01775			
3rd measured cross-section (curve segment)	34.92	1st cutting pass	30.099(1)	30.042(1)	0.189%	21.379	0.342(1)	0.331(1)	0.01775	201.688	201.629	0.029%
	19.88	2nd cutting pass	30.216(2)	30.146(2)	0.232%		0.424(2)	0.435(2)	0.01775			
4th measured cross-section (curve segment)	34.92	1st cutting pass	30.081(1)	30.025(1)	0.186%	21.537	0.36(1)	0.352(1)	0.01775	201.756	201.700	0.028%
	19.88	2nd cutting pass	30.158(2)	30.097(2)	0.202%		0.421(2)	0.424(2)	0.01775			
5th measured cross-section (curve segment)	34.92	1st cutting pass	30.083(1)	30.025(1)	0.193%	21.704	0.379(1)	0.370(1)	0.01775	201.878	201.833	0.022%
	19.88	2nd cutting pass	30.136(2)	30.072(2)	0.212%		0.410(2)	0.417(2)	0.01775			

Remarks: Cutting depth (1) represents the cutting depth at the 1st cutting pass.
Cutting depth (2) represents the cutting depth at the 2nd cutting pass.
Protruding height value (1) represents the protruding height value from the point of protruding height between the 1st cutting pass and the 2nd cutting pass to the bottom at the 1st cutting pass.
Protruding height value (2) represents the protruding height value from the point of protruding height between the 1st cutting pass and the 2nd cutting pass to the bottom at the 2nd cutting pass.

As seen from the difference between simulation results and experimental results shown in Table 1, the difference in cutting depth in Table 1 is smaller than 0.3%; the difference in width of opening in the Table 1 is smaller than 0.025%; and the difference in upward height in the Table 1 is smaller than the target convergence value 0.54nm. Therefore, it is proved that the paper's simulation model and AFM machining experimental method of nanochannel that integrates straight line segment machining with Cubic Spline curve segment machining to the expected depth and expected width is feasible. The diagrams below show some the measurement results of AFM experiment, as shown in Figure 12 to Figure 13. These figures prove that the experimental data shown in Table 1 are acquired in AFM experiment.

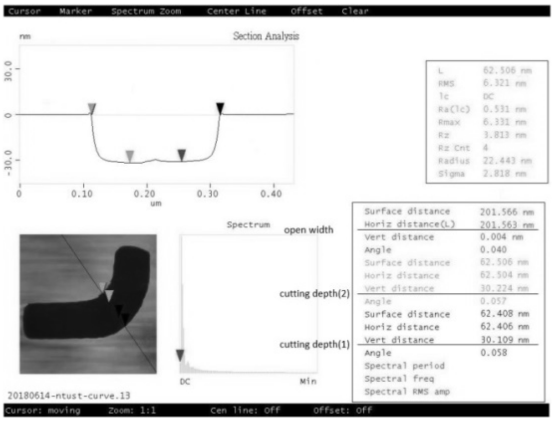

Figure 12 Diagram of experimental measurement of the width of opening and cutting depths of the 2nd measured cross-section (Cubic Spline curve segment) on the 2nd cutting layer at two cutting passes under the expected depth 30nm and the expected width 202nm

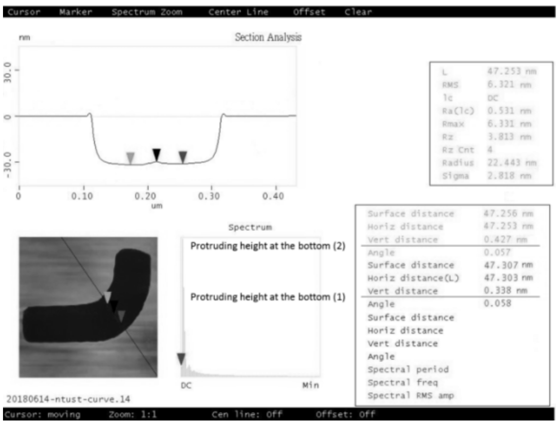

Figure 13 Diagram of experimental measurement of the upward heights of the 2nd measured cross-section (Cubic Spline curve segment) on the 2nd cutting layer at two cutting passes under the expected depth 30nm and the expected width 202nm

CONCLUSION

The paper proposes the simulation model and the AFM machining experimental method of trapezium groove on nanochannel that integrates straight line segment with Cubic Spline curve segment to the expected depth and the expected width.

When calculating the Cubic Spline curve segment, the paper proposes a simulation model of nanochannel Cubic Spline curve machining to the expected width and expected depth. First of all, the paper uses cubic spline Cubic Spline curve equation acquired from the self-set control points to calculate multiple tiny straight line segments, with integers taken, of approximate Cubic Spline curve in order to carry out AFM straight line segment and Cubic Spline curve machining experiment.

The paper also innovatively proposes using the control points set by the first Cubic Spline curve, and then uses offset equation and the offset amount acquired by the above way to find the calculation method of the control points of Cubic Spline curve equations of other cutting passes on the same cutting layer. Furthermore, the paper calculates the Cubic Spline curve equations of other cutting passes on the same cutting layer. Since AFM machine cannot carry out Cubic Spline curve machining, the paper proposes applying the calculation equations of the chord height tolerance of Cubic Spline curve and tiny straight line segment. In times of measurement we take the cross-section at the positions of the approximate ideal Cubic Spline curve for measurement. Finally, the simulation results of the simulation model established by the paper that integrates straight line segment machining with Cubic Spline curve segment to the expected depth and expected width, are compared to the experimental results, proving that the simulation model established by the paper is feasible and acceptable.

ACKNOWLEDGMENT

The authors thank the Ministry of Science and Technology of Taiwan (grant number MOST 109-2221-E-011-004-) for its support of this research.

REFERENCES

Binning, G., Quate, C. F. and Gerber, C., "Atomic Force Microscope", Physical Review Letters, Vol. 56, No. 6, pp.930-933 (1986).

Cardoso, V. F., Mirandaa, D., Botelhoc, G., Minasb, G. and Lanceros-Méndeza, S., "Highly effective clean-up of magnetic nanoparticles using microfluidic technology", Sensors and Actuators B, Vol. 255, pp. 2384–2391 (2018).

Fang, T. H., Weng, C. I. and Chang, J. G., "Machining Characterization of Nano-lithography Process by Using Atomic Force Microscopy", Nanotechnology, Vol. 11, No. 5, pp. 181-187 (2000).

Lübben, J. F. and Johannsmann, D., "Nanoscale High-frequency Contact Mechanics Using an AFM Tip and a Quartz Crystal Resonator", Langmuir, Vol. 20, No. 9, pp. 3698-3703 (2004).

Lin, Z. C. and Hsu, Y. C., "A calculating method for the fewest cutting passes on sapphire substrate at a certain depth using specific down force energy with an AFM probe", Journal of Materials Processing Technology, Vol. 212, pp. 2321-2331 (2012).

Lin, Z. C. and Yang, C. B., "Cubic Spline curve Fabrication Model analysis of Near Fiald Photolithography", Proceedings of the Institution of Mechanical Engineers, Part B, Journal of Engineering Manufacture Vol. 225, pp. 663-674 (2011).

Nanjo, H., Nony, L., Yoneya, M. and Aime, J. P., "Simulation of Section Cubic Spline curve by Phase Constant Dynamic Mode Atomic Force Microscopy in Non-contact Situation", Applied Surface Science, Vol. 210, No. 1, pp. 49-53 (2003).

Schumacher, H. W., Keyser, U. F. and Zeitler, U., "Controlled mechanical AFM fabrication of two-dimensional electron systems: Fabrication of a single-electron transistor", Physica E., Vol. 6, pp. 860-863 (2000).

Tseng, A. A., Jou, S., Notargiacomo, A. and Chen, T. P., "Recent Developments in Tip-based Nanofabrication and Its Roadmap", Journal of Nanoscience & Nanotechnology, Vol. 8, No. 5, pp. 2167–2186 (2008).

Yongda, Y., Tao, S., Liang, Y. C. and Shen, D., "Investigation on AFM based micro/nano CNC machining system", International Journal of Machine Tools and Manufacture, Vol. 47, No. 11, pp.1651-1659 (2007).

Yeh, S. S. and Hsu, P. L., "Adaptive-feedrate Interpolation for Paramertic Cubic Spline Cubic Spline curves with a Confined Error" Computer-Aided Design, Vol. 34, pp. 229-237 (2002).

單晶矽奈米流道三次樣條曲線加工之模擬模式建立及實驗驗證

林榮慶 方信人 何杰珉
國立台灣科技大學 機械工程系

摘要

本文提出奈米流道三次樣條曲線加工到預定寬度及深度之模擬模式，並進行 AFM 的直線段與曲線加工實驗驗證。本文先利用加工直線梯型凹槽到預定深度及寬度的方法，算出加工直線梯型凹槽到預定深度及寬度所需的偏移量以及用比下壓能法算出切削道次數。然後利用自行設定的控制點取得欲加工路徑的三次樣條曲線方程式。本文亦創新提出，利用第一條三次樣條曲線所設立的控制點，再利用偏移公式以及上述所求出的偏移量，求出同一切削層其他切削道次的三次樣條曲線方程式的控制點的計算方法，進而計算出同一切削層其他切削道次的三次樣條曲線方程式。由於 AFM 機台無法進行三次樣條曲線加工，故本文提出應用三次樣條曲線與微小線段的弦誤差的計算公式，進而用直線近似三次樣條曲線的方法算出由許多微小線段連結而成的近似三次樣條曲線之直線。又因為 AFM 機台精度只到 1nm，故我們將微小線段的各個交點取整數來進行加工，而為縮小誤差，我們在進行量測時取近似理想三次樣條曲線位置的斷面進行量測。最後進行本文所建立的三次樣條曲線加工到預定寬度及深度之模擬模式的模擬結果與實驗結果相比較，驗證本文所建立之模擬模式為合理可接受的。